Cytometry 40:88–101 (2000)

Original Articles

Polarization of Scatter and Fluorescence Signals in Flow Cytometry

Charles L. Asbury, Jeanne L. Uy, and Ger van den Engh*
Department of Molecular Biotechnology, University of Washington, Seattle, Washington

Received 1 November 1999; Revision Received 31 January 2000; Accepted 16 February 2000

Background: The pulses of light scatter and fluorescence measured in flow cytometers exhibit varying degrees of polarization. Flow cytometers are heterogeneously sensitive to this polarization, depending on the light source(s), the optical layout, and the types of mirrors and filters used. Therefore, fluorescence polarization can affect apparent intensity ratios between particles and interfere with schemes for interlaboratory standardization.
Methods: We investigate the degree to which polarization affects common flow cytometry measurements. Our technique for determining polarization differs from previous methods because complete distributions of intensity versus polarization angle are measured, rather than intensities at just two orthogonal polarization angles. Theoretical models for scatter and fluorescence are presented and verified by making polarization measurements of calibration beads.
Results: Measurements of cells stained with a variety of dyes illustrate that fluorescence polarization occurs frequently in flow cytometry.
Conclusions: Consequences for quantitative cytometry are discussed, and the use of the "magic angle" to make a flow cytometer insensitive to fluorescence polarization is proposed. Cytometry 40:88–101, 2000.

Key terms: fluorescence polarization; anisotropy; transition dipole; fluorescein (FDA, FITC); phycoerythrin (PE); thiazole orange (TO); ethidium bromide (EB); propidium iodide (PI); TOTO-1; ethidium homodimer (ETHD-2); YOYO-1; quantitative flow cytometry (QFCM)

Light has three qualities: color, intensity, and polarization. In cytometry, we are usually concerned with the first two properties only. We select color with a suitable filter and measure the intensity of light that passes the filter. The polarization of the light is usually ignored, despite the fact that the intensity measurement may depend on the degree and direction of polarization. Most cytometers are (unintentionally) polarization sensitive. Therefore, the apparent intensity of a light source can be changed by rotating the detection optics around the collection axis. Of even greater consequence is the fact that polarization of a fluorescent source is an indication of anisotropy: the object emits different amounts of light in different directions. Two identical detectors looking at the same object from different vantage points may give different light intensity readings. With anisotropic light emission and polarization-sensitive detectors, the question, "How bright is the particle?" has an ambiguous answer. Avoiding this ambiguity requires specifying the polarization state of the incident light, the direction of observation, and the orientation and polarization sensitivity of the detector. Ideally, one would present the complete angular distributions of intensity and polarization emitted by an object of interest. Such detailed specifications of experimental conditions and results are not commonly practiced by the flow cytometry community.

A cavalier treatment of polarization would be justified if anisotropy played no role in flow measurements.

Clarification of terms: degree of polarization: quantitative measure of the amount of polarization, *P* value; direction of polarization: the direction of the electric field of a photon; polarization state: refers to both the degree and direction of polarization; emission anisotropy: total emission is different depending on the direction of observation; anisotropy in the distribution of dipoles: distribution of dipoles is not spherically symmetric.

Grant sponsor: NSF Science and Technology Center; Grant number: BIR 9214821; Grant sponsor: NIH; Grant number: T32 GM00035-05.

*Correspondence to: Ger van den Engh, Department of Molecular Biotechnology, University of Washington, Box 357730, Seattle, WA 98195-7730.
E-mail: engh@biotech.washington.edu

However, there are good reasons to suspect that flow cytometry is affected by anisotropy. Flow cytometry almost exclusively employs coherent, highly polarized light sources, so the scatter and fluorescence pulses measured in flow experiments are very likely to be anisotropic. In the few cases where investigators have looked for fluorescence polarization, it has been observed. Early measurements of polarization in a flow cytometer were made by Arndt-Jovin et al. (1,2). They originally used the method to observe changes in the rotational freedom of membrane-bound dyes (i.e., membrane fluidity). Later (3), they used the method to verify the occurrence of energy transfer between labeled cell-surface receptors. Other investigators have used similar methods to measure the fluorescence polarization of intracellular fluorescein (4–7) and of various DNA- and membrane-bound dyes (8–15), because polarization provides information on the cellular context of these molecules. Measurements of fluorescence polarization of peripheral blood cells have been reported to be useful for the study and diagnosis of cancer (16) and Alzheimer's disease (17). Besides these experiments, which deliberately aimed to induce and utilize signal polarization, there are few observations of polarization under "normal" conditions. The degree to which anisotropy occurs in ordinary flow experiments is not documented.

Anisotropy, if it occurs, introduces an arbitrary element in scatter and fluorescence measurements. Calibration of detectors, instruments, reagents, and fluorescence standards has been a long-time (and somewhat elusive) goal of the flow community. With anisotropy, two instruments can yield different results, and both can be right. The converse is also true. If machine parameters are adjusted until two supposedly identical experiments yield the same results, artifacts such as offsets and nonlinearities may be introduced. It is clear that we need to know how prevalent anisotropy of scatter and fluorescence is before flow measurements can be truly standardized.

In order to determine the extent to which cytometric measurements are affected by anisotropy, we need a theory and adequate measurement tools. This manuscript presents simple theoretical models for scatter and fluorescence that predict how the polarization and emission anisotropy for these signals depend on experimental conditions. A simple method to measure polarization is described. It requires minimal modification of a flow cytometer. We then present measurements of calibration beads to show that polarization in flow cytometry follows the qualitative and quantitative predictions of the models. Cells stained with a variety of common flow cytometry dyes exhibited some degree of fluorescence polarization for all the dyes tested; in many cases, the degree of polarization was quite high. These results indicate that anisotropy is the rule rather than the exception and that this source of nonlinearity must be considered, determined, and eliminated before standardization of flow measurements becomes feasible.

THEORY

Different mechanisms are responsible for the anisotropy of scatter and fluorescence. Although geometrically complex, the scattering of polarized light by small transparent particles is described well by the rules of classical optics: reflection, refraction, diffraction, and interference. In contrast, the light-matter interactions that lead to fluorescence must be analyzed at the molecular level. These considerations lead to different predictions for the anisotropy of fluorescence and scatter signals that can be tested by experiment.

The following section describes the physical processes that cause light scattering and fluorescence emission using simple models. It will be shown that, under conditions typical in flow cytometry, both scatter and fluorescence are anisotropic, exhibiting significant variations in intensity with both the angle of observation and the polarization sensitivity of the detector. The models are then used to make quantitative predictions about the direction and degree of polarization expected in flow experiments.

Angular Distribution of Scattered Light

When a laser beam hits a small particle, incident light is scattered unequally in many directions. The intensity of the scatter at a given angle of observation depends mainly on the properties of the particle: its refractive index, its shape, and especially its size. Transparent particles that are much larger than the wavelength of the illumination behave like lenses, so that their scatter distribution can be derived from simple rules of reflection and refraction. For smaller particles, the effects of diffraction and the associated constructive and destructive interference must also be included. Consequently, the scatter from microscopic objects may have very complicated, multi-lobed angular distributions. Theoretical calculations can successfully predict these distributions for objects with simple shapes and homogeneous refractive indices (18). However, biological cells are uniform and homogeneous by approximation only, often having rough surfaces and complex internal structures. Furthermore, in flow cytometry, cells have an uncertain orientation and are observed in motion and the illumination beam and scatter distribution are distorted by the fluid jet and other optical components. Theoretical calculations incorporating all these effects would be accurate but impractically cumbersome. Thus, although the physical mechanisms of light scattering are well understood, theoretical predictions about scatter signals from individual cells in flow cytometry are approximations that must be verified by experimentation.

Theory, supported by empirical observation, has led to useful generalizations about the angular distribution of scattered light. It has been established that scatter signals collected over wide angles can be used to discriminate between different cell types. When scatter signals are integrated over wide ranges of angles, the peaks and valleys in the angular distributions tend to cancel each other and useful trends emerge. Forward scatter integrated over angles between 1.5° and 15° with respect to

the incident beam is roughly proportional to the cross-sectional area of the particle. The perpendicular scatter collected between 80° and 100° is high for structurally complex cells, such as those with nonspherical shapes or refractive cytoplasmic structures. Integrated forward and perpendicular scatter signals measure complimentary properties and form the basis for distinguishing between certain cell types, such as bone marrow cells, in scatter plots (19).

Scatter Polarization Is a Direct Reflection of the Incident Polarization

The polarization state of light scattered from small particles can also be understood using the principles of classical optics. Unlike intensity, the polarization state of light scattered toward a given angle of observation can be predicted easily and accurately with these simple rules.

Any interface between two media of different refractive index is partially reflective. Therefore, the cell membrane and the organelles inside a cell present many convoluted and potentially reflective surfaces. For a given scattering angle, there will always be some surfaces oriented appropriately to reflect light toward that direction (somewhat like a dance club "disco ball," except that the reflections are partial and the mirrors are nonmetallic). The light scattered toward one direction is a superposition of all the light reflected one or more times from appropriately oriented surfaces. In most cells, the surfaces are only weakly reflective. In addition, most of the scattered light observed at a given angle will have undergone just a single reflection from parallel surfaces (multiple reflection events representing only a small fraction of the total scattered intensity). Single reflections of this kind preserve the high degree of polarization of the incident laser beam, so the scatter will appear highly polarized from any viewing direction. If the plane containing the illumination beam and the axis of detection is taken as a reference, then the polarization vector of the detected scatter will make the same angle as the incident polarization with this plane. Note that the polarization vector of the scatter will rotate around the detection axis when the plane of observation is changed, or equivalently, when the polarization of the incident beam is turned.

Most surfaces in a cell reflect only a very small fraction of the incident light. We present data below showing that this single-reflection model predicts reasonably well the polarization state of scatter from beads and structurally simple cells (mouse thymocytes). However, some cells have highly reflective internal structures for which multiply-reflected scatter represents a more significant fraction of the total. Multiple reflection rotates the polarization of some of the scattered light in a compound manner, reducing the overall degree of polarization of the scatter. Indeed, scatter depolarization has been used to separate eosinophils from neutrophils— cells that contain granules that differ in refractivity (20).

Quantitative Predictions About Scatter Polarization

A laser with perfect vertical polarization emits only light waves with vertical electric fields. A polarizing prism in front of this source will pass the (vector) component of the field that is aligned with its pass-axis. Therefore, if η is the angle between the pass-axis of the prism and vertical, the intensity of light passing through the prism will be proportional to $\cos^2\eta$. (The square occurs because light intensity is proportional to the square of the electric field strength.) Note that a perfectly polarized source can be completely extinguished if the pass-axis is orthogonal to its direction of polarization ($\cos^2 [90°] = 0$).

The single-reflection model predicts that scattering should preserve the high degree of polarization of the incident laser and that the direction of polarization will rotate around the detection axis if the plane of observation (defined above) is changed, or equivalently, if the laser polarization is turned. Therefore, the scatter intensity, I, should vary with the pass-angle of the polarizer, η, according to

$$I(\eta) = \alpha \cdot \cos^2(\eta - \gamma). \quad (1)$$

Here α represents the intensity that would be measured without a polarizer and η is measured relative to vertical. The constant γ is included to account for possible rotation of the scatter polarization. (In a conventional cytometer, $\gamma = 0$, because the incident laser is polarized vertically, and scatter is measured in the horizontal plane.)

Fluorescence Anisotropy Occurs Through Photoselection

Like scatter, the fluorescence induced by a polarized light source is polarized and is not emitted with equal intensity in all directions. However, unlike scatter, the polarization of fluorescence is never complete. Furthermore, fluorescence polarization cannot be understood without considering some details of the interactions between photons and fluorescent molecules.

To produce fluorescence, a dye molecule must first become electronically excited through the absorption of a photon. An electron is elevated from its ground state into a higher energy orbital, where it stays for a short time— the excited-state lifetime (typically about 10 ns)— before returning to the ground state and emitting a fluorescence photon. Each of these electronic transitions absorbs or creates a photon with a preferred direction of polarization. The reason for this preference is simple. While undergoing an electronic transition, the electron cloud (technically, the electron wave function) vibrates in a certain direction with respect to the molecular structure. Depending on whether the transition is an absorption or emission, the direction of vibration is called the absorption- or emission-transition dipole moment of the molecule. Just as in a radio antenna, absorptions are most likely if the electric field of the photon is aligned with the absorption-transition dipole. Similarly, emitted photons will tend to have their electric fields aligned with the

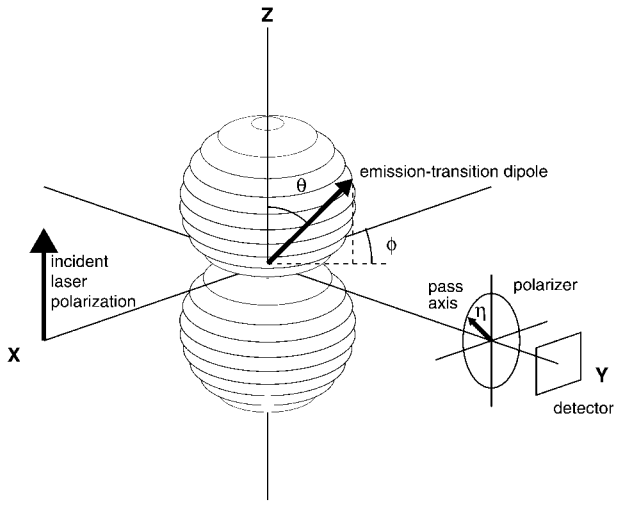

FIG. 1. Schematic drawing of the distribution of fluorophores excited by a polarized laser. Incident light propagates along the *x*-axis and is polarized along the *z*-direction. The resulting population of emitting fluorophores will be nonrandom and cylindrically symmetric about the *z*-axis. The orientation of an individual fluorophore within this distribution is specified by the angles θ and ϕ. The length of the vector extending from the origin to the surface at (θ, ϕ) represents the number of emitting dipoles with that orientation. Fluorescence emitted in the *y*-direction is detected after passing through a polarizer with its pass-axis at an angle η with respect to the *z*-direction.

emission-transition dipole. The absorption and emission dipoles are fixed relative to the molecular structure and can be (at least roughly) predicted using principles of quantum mechanics. The absorption and emission dipoles are parallel for many fluorophores, but in some cases they can be misaligned from one another.

When a vertically polarized laser beam (i.e., a stream of photons with electric fields all pointing up) hits a collection of randomly oriented dye molecules, photoselection occurs. Molecules with absorption-transition dipoles that happen to be nearly vertical are preferentially excited. As depicted in Figure 1, the resulting distribution of excited fluorophores is cylindrically symmetric and it contains many molecules with vertical or near-vertical absorption dipoles. It contains no molecules with horizontal absorption dipoles. When this collection of molecules emits fluorescence, the distribution of emitting dipoles will also be anisotropic and cylindrically symmetric.

Cylindrical symmetry in the distribution of emitting dipoles has important consequences: Collectively, such dipoles will produce fluorescence that appears partially polarized when viewed from any direction except along the axis of cylindrical symmetry (i.e., the vertical, or *z*-axis of Fig. 1). The degree of polarization will be highest when the detection axis is perpendicular to the axis of symmetry and will decrease to zero as the detection axis is brought in-line with the symmetry axis. Because light waves (photons) travel in a direction perpendicular to their polarization direction, the total fluorescence intensity will vary in analogous fashion. The maximum total intensity will be found where the detection axis is perpendicular to the symmetry axis. A minimum intensity will occur when the detector is located on the symmetry axis.

The degree of anisotropy in the population of emitting dipoles will vary with properties of the fluorophores. The maximum possible anisotropy will occur when (1) the fluorophores cannot rotate significantly during the lifetime of the excited state, (2) energy transfer between fluorophores is not occurring, and (3) the absorption and emission dipoles of the fluorophores are parallel. In this special case (which is treated mathematically below), the distribution of emitting dipoles is equivalent to the distribution of excited absorption dipoles. In general, rotation due to Brownian motion during the excited state lifetime and energy transfer tend to randomize the orientation of emitting dipoles, making their distribution more isotropic. Misalignment of the absorption- and emission-transition dipoles also alters the distribution of emitting dipoles, but does not necessarily randomize it. For example, if the angle between absorption and emission dipoles is 90°, the distribution may contain few (or no) emitting dipoles that are aligned with the excitation. It is, therefore, theoretically possible for a vertically polarized laser to generate horizontally polarized fluorescence.

Quantitative Predictions About Fluorescence Polarization

As described above, photoselection causes fluorescence emission to be polarized, but never completely. Light waves emitted from a partially polarized source have electric fields that are aligned, but the alignment is imperfect. Viewed through a polarizing prism, the intensity of such a source will be minimized when the pass-axis is orthogonal to the direction of polarization, but it will not be completely extinguished. The imperfect alignment of the electric fields ensures that for every orientation of the prism, there will be at least some light with an electric field component along its pass-axis. The following analysis (adapted from ref. 21) shows that fluorescence intensity should vary with the pass angle of the polarizer, η, according to

$$I(\eta) = \alpha \cdot \cos^2\eta + \beta \cdot \sin^2\eta, \qquad (2)$$

where α and β are the intensities measured when the pass-axis is vertical and horizontal, respectively. The total intensity that would be measured without a polarizer is (α + β). As will be shown, the photoselection process imposes theoretical limits on the relative magnitudes of α and β.

The probability that a laser polarized along the *z*-axis will excite a particular fluorophore is proportional to $\cos^2(\theta)$, where θ is the (azimuthal) angle between the absorption-transition dipole of the fluorophore and the *z*-axis (Fig. 1; 21). If a collection of randomly oriented fluorophores is illuminated, then the fraction of excited molecules having orientations within the interval θ to θ + dθ and ϕ to ϕ + dϕ is given by

$$W(\theta, \phi)d\theta\ d\phi = \frac{3}{4\pi}\cos^2\theta \sin\theta\ d\theta\ d\phi, \qquad (3)$$

where ϕ is the equatorial angle (Fig. 1). The factor $\sin\theta$ is necessary because there are many more possible orientations, and hence more molecules in our random collection, near horizontal ($\theta \sim 90°$) than near vertical ($\theta \sim 0°$). The normalization factor $3/4\pi$ is defined by

$$\int_0^{2\pi} d\phi \int_0^{\pi} d\theta W(\theta, \phi) = 1. \qquad (4)$$

For simplicity, only fluorophores with parallel absorption and emission dipoles will be considered, and fluorophore rotation and energy transfer will be assumed not to occur. (Although rarely found in real experiments, this situation is an important limiting case that gives the maximum possible anisotropy.) With these assumptions, the distribution of emitting dipoles is equivalent to the distribution of excited dipoles.

The total emission from the population is calculated by summing the contributions from molecules in every possible orientation. Light emitted from a single, stationary fluorophore is perfectly polarized. Thus (as explained above), the intensity passing through a polarizer will be proportional to $\cos^2\xi$, where ξ is the angle between the emission-transition dipole of the fluorophore and the pass-axis. If the pass-axis makes an angle η with the vertical, then $\cos^2\xi$ can be expressed as a function of θ and ϕ using a simple trick. The unit vectors

$$\hat{\mu} = \hat{i}\sin\theta\cos\phi + \hat{j}\sin\theta\sin\phi + \hat{k}\cos\theta \quad \text{and} \qquad (5)$$

$$\hat{q} = \hat{i}\sin\eta + \hat{k}\cos\eta \qquad (6)$$

represent the orientations of the emitting dipole and the pass-axis, respectively. (Note that $\hat{q}$ is chosen, arbitrarily, to be in the *x*-*z* plane. Because of cylindrical symmetry, the calculated results do not depend on this choice.) Both vectors have unit length, so that their dot product will be equal to the cosine of the angle between them (22), giving

$$\cos^2\xi = (\hat{\mu}\cdot\hat{q})^2 = (\sin\eta\sin\theta\cos\phi + \cos\eta\cos\theta)^2. \qquad (7)$$

The relative intensity seen through the polarizer is now obtained by multiplying Equation 3, the fraction of molecules in a given orientation, by Equation 7, the contribution from those molecules, and integrating over all possible orientations,

$$I(\eta) \propto \int_0^{2\pi} d\phi \int_0^{\pi} d\theta\ \cos^2\xi\ W(\theta, \phi). \qquad (8)$$

Note that only the variation of I with η is calculated here. (To obtain the actual measured intensity, Equation 8 must be scaled by the illumination intensity, the absorption cross-section and quantum efficiency of the fluorophores, and the light collection efficiency of the measuring instrument.) Expanding $\cos^2\xi$ and $W(\theta, \phi)$ and rearranging gives

$$I(\eta) \propto \frac{3}{4\pi}\sin^2\eta \int_0^{2\pi} d\phi\ \cos^2\phi \int_0^{\pi} d\theta\ \cos^2\theta \sin^3\theta$$

$$+ \frac{3}{4\pi}\cos^2\eta \int_0^{2\pi} d\phi \int_0^{\pi} d\theta\ \cos^4\theta \sin\theta \qquad (9)$$

$$+ \frac{6}{4\pi}\sin\eta\cos\eta \int_0^{2\pi} d\phi\ \cos\phi \int_0^{\pi} d\theta\ \cos^3\theta \sin^2\theta.$$

Performing the integrations gives the final result,

$$I(\eta) \propto \frac{3}{5}\cos^2\eta + \frac{1}{5}\sin^2\eta, \qquad (10)$$

which is plotted in Figure 2A.

It is instructive to compare Equation 10 to the result that would be obtained for a completely isotropic distribution of fluorophores. For the isotropic case,

$$W(\theta, \phi)d\theta\ d\phi = \frac{1}{4\pi}\sin\theta\ d\theta\ d\phi \qquad (11)$$

Inserting Equation 11 into Equation 8 and integrating confirms that the intensity is the same for all polarization angles,

$$I(\eta) \propto \frac{1}{3}\cos^2\eta + \frac{1}{3}\sin^2\eta = \frac{1}{3}. \qquad (12)$$

Equations 10 and 12 are specific forms of the more general Equation 2. If $\beta = 0$, Equation 2 describes a source with perfect vertical polarization (i.e., along the *z*-axis in Fig. 1). If $\alpha = 0$, the source has perfect horizontal polarization (along the *x*-axis in Fig. 1). Evidently, the partially polarized case, Equation 10, and even the unpolarized case, Equation 12, can be thought of as a weighted sum of these two components. Strictly, however, a third component is missing in Equations 2, 10, and 12. The missing component is polarized directly along the detection axis (the *y*-axis in Fig. 1), and therefore does not propagate toward the detector. Because of cylindrical symmetry, the two horizontal components (*x*- and *y*-) must be equal. Thus, even though it is not measured, the missing component is known. (Note that the coefficients in Equations 10 and 12 do not quite add up to one. The missing fraction in each case is equal to the coefficient of $\sin^2\eta$. Also note that a detector located on the *z*-axis would receive the two equal *x*- and *y*-polarized components, which add together to make unpolarized light.)

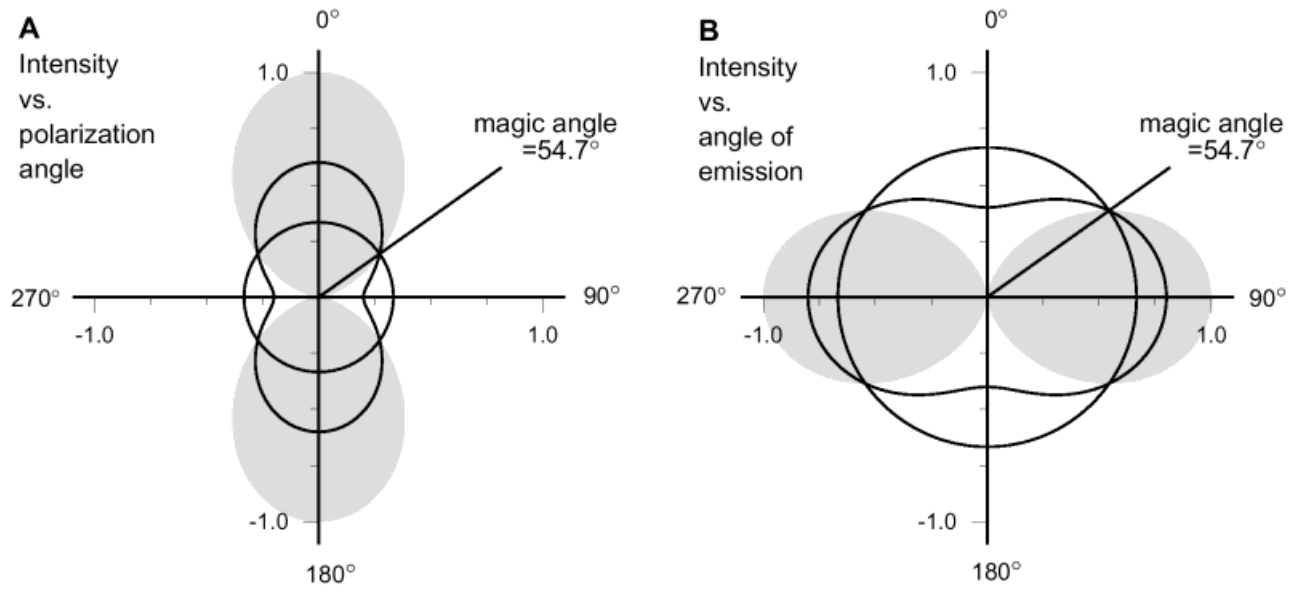

FIG. 2. Polar plots of predicted fluorescence intensity variations. In these plots, intensity is represented by the radial distance from the origin and the angle is measured clockwise from the vertical axis. **A:** The variation of fluorescence intensity with polarization angle is shown for the isotropic case (Equation 12, black circle) and the maximally anisotropic case (Equation 10, bean-shaped curve). The perfectly polarized case, $I(\eta) = \cos^2\eta$, which cannot occur with fluorescence, is also shown for comparison (shaded gray). Note that a polarizer oriented at $\eta = 54.7°$ would pass the same intensity regardless of the degree of fluorescence anisotropy. **B:** The variation of fluorescence intensity with angle of emission is shown for the isotropic case (Equation 14, black circle) and the maximally anisotropic case (Equation 13, bean-shaped curve). The perfectly polarized case, $I_{OA}(\eta) = \sin^2\eta$, which cannot occur for fluorescence, is also shown for comparison (shaded gray). A detector that collects only the light emitted along $\eta = 54.7°$ would detect the same intensity regardless of the degree of fluorescence anisotropy.

Angular Distribution of Fluorescence

The mathematics leading to Equations 10 and 12 can also be used to determine how the total fluorescence intensity (measured without a polarizer) varies as the angle of observation is changed. In this case, the symbols η and ξ are taken to represent the angle between the detection axis and vertical (η), and that between the detection axis and the emission-transition dipole (ξ). With these substitutions, the derivation is exactly the same as that for Equations 10 and 12, with one exception: The emission intensity from a single, stationary fluorophore is proportional to $\sin^2\xi = 1 - \cos^2\xi$, so that this quantity is used in place of Equation 7. Multiplying $\sin^2\xi$ by Equation 3 and integrating over all angles gives the variation of intensity with angle of observation for a maximally anisotropic fluorescent source,

$$I_{OA}(\eta) = \frac{2}{5}\cos^2\eta + \frac{4}{5}\sin^2\eta. \qquad (13)$$

An isotropic source is treated by multiplying $\sin^2\xi$ by Equation 11 and integrating,

$$I_{OA}(\eta) = \frac{2}{3}\cos^2\eta + \frac{2}{3}\sin^2\eta = \frac{2}{3}, \qquad (14)$$

confirming that fluorescence intensity in this case does not vary with the observation angle. Equations 13 and 14 are plotted in Figure 2B.

At the "Magic Angle" Fluorescence Intensity Is Independent of Polarization State

The preceding analysis shows that fluorescence intensity measured at an arbitrarily chosen polarization angle, or at an arbitrary observation angle, will depend on the degree of anisotropy in the distribution of emitting dipoles. However, inspection of Figure 2A,B indicates that it is possible to make intensity measurements that are independent of anisotropy, by choosing $\eta = 54.7°$. Measured intensity is proportional to the total emission, regardless of anisotropy, when either (1) a polarizer with pass-axis at $\eta = 54.7°$ is placed in front of the detector, or (2) the detector collects only light that is emitted in a direction $\eta = 54.7°$ from the direction of laser polarization. (It should be noted that 54.7° is the proper angle only when a linearly polarized laser is used. For a circularly, or randomly, polarized beam, the situation will be different because the propagation direction of the incident light, rather than its direction of polarization, will become the axis of cylindrical symmetry.) Time-resolved cuvette fluorometry measurements are sometimes performed with a polarizer at this so-called magic angle in front of the detector, so that measured fluorescence lifetimes are unaffected by anisotropy (23).

Quantifying Polarization State Using *P*

Distributions of intensity versus polarization angle, $I(\eta)$, are not often measured because the polarization state can be unambiguously specified by intensities at just two an-

gles, $I(0°) = \alpha$ and $I(90°) = \beta$, provided that the direction of polarization of the source is known a priori. Often, the degree of polarization is summarized using the following quantity:

$$\text{Polarization} = P = (\alpha - \beta)/(\alpha + \beta) \qquad (15)$$

P is a normalized quantity that evaluates to unity for perfectly polarized light and zero for unpolarized light. As explained above, Equation 10 represents the maximum possible fluorescence polarization, so that P must be ≤ 0.5 for any fluorescence emission.

When the direction of polarization of a source is not known in advance, the angles corresponding to $\eta = 0°$ and $\eta = 90°$ are unknown. In this case, the distribution of intensity versus polarization angle, $I(\eta)$, must be measured in order to find the main axis of polarization from which η is defined. Measuring $I(\eta)$ over a range of angles also provides better physical insight and more rigorous testing of the models described above.

Testable Hypotheses

If the foregoing theory applies to the polarization of light pulses in flow cytometry, then we should observe the following:

1. Distributions of intensity versus polarization angle for all measurements should fit well with Equation 2.

2. Scatter should be highly polarized, i.e., $P \sim 1$. The main direction of scatter polarization should rotate if the laser polarization is turned.

3. Fluorescence should be partially polarized, with $P \leq 0.5$. The degree of fluorescence polarization should be maximum when the laser is polarized perpendicularly to the detection axis. Turning the laser polarization so that it is parallel to the detection axis will place the detector on the symmetry axis of the population of emitting dipoles. In this case, the collected fluorescence will be unpolarized ($P \sim 0$).

MATERIALS AND METHODS

Flow Cytometer

All measurements were performed using a flow cytometer designed and developed in this laboratory (24,25). Fluidic and optical components were mounted on an optical bench, allowing easy access to and modification of the instrument. A 70-μm nozzle operating at 210 kPa (30 psi) produced a jet velocity of ~20 m/s. Samples were injected into the center of the stream through a PEEK capillary tube (Upchurch, Oak Harbor, WA) with an internal diameter of 250 μm. Two argon lasers were used, which were tuned for multiline UV (model Innova 307; Coherent, Santa Clara, CA) and single-line visible excitation (model Innova 306). Typically, the lasers were adjusted to produce 100 mW or less. Lasers were usually polarized vertically, parallel to the jet, except in a few experiments when the laser polarization was rotated using a half-wave retarder.

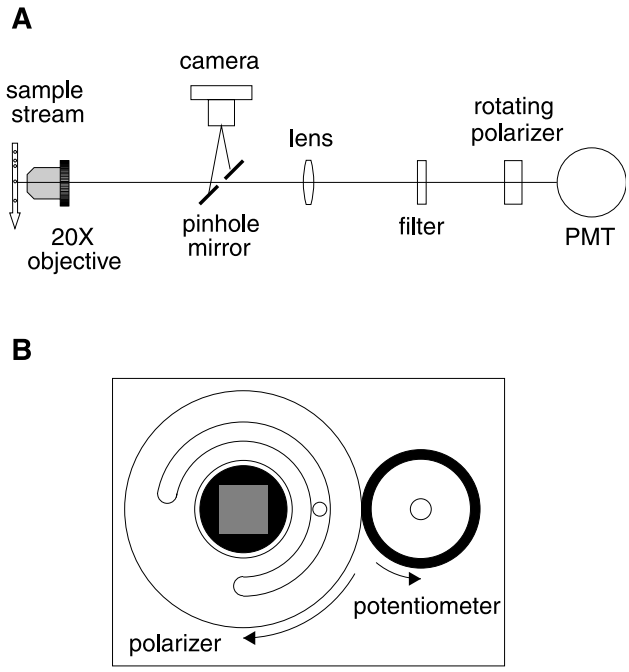

FIG. 3. Diagram of signal collection optics and polarizer. **A:** A 20× microscope objective focused light from the measurement point onto a pinhole mirror. Light reflected off the mirror was imaged with a CCD camera, allowing continuous inspection of the instrument alignment. Light passing through the pinhole was collimated by a lens before passing through color filters, the polarizer, and onto a photomultiplier (PMT). **B:** Front view of the polarizer and potentiometer. The polarizer was mounted in the center of a rigid wheel that rotated 260°. A rubberized wheel on the potentiometer contacted the outer diameter of the potentiometer wheel, so the two rotated simultaneously (indicated by arrows). The potentiometer provided a voltage that was linearly related to the angle of the polarizer.

Light emitted from the laser crossing-point was focused onto a pinhole mirror (Fig. 3A) using an objective lens with 0.42 NA (20× M Plan Apo, model 378-804-2; Mitutoyo, Japan). At this low numerical aperture, aperture depolarization effects are expected to be minimal (7,26). The pinhole acted as a spatial filter. Light passing through the pinhole was collimated by a lens (f = 75 mm) before passing through color filters and entering the polarizer (described below). Light reflected by the pinhole mirror was imaged onto a CCD camera and displayed on a video monitor, allowing continuous visual inspection of the alignment of stream, laser, and pinhole.

The electronics of the machine have been described previously (25). The system can accept up to eight input signals. The inputs can either measure DC levels or pulse heights. Pulsed inputs are filtered using baseline-restoration circuitry before analog-to-digital (A/D) conversion to remove background from the pulsed light signals coming from measured particles. DC inputs are used to record continuous signals in the data list (e.g., laser power [27], temperature, or other externally varying parameters [24]) and are fed directly into A/D converters without baseline-restoration. In this study, the angle of the polarizer was voltage encoded and stored using one of the DC inputs.

Attachment of Polarizer

A Glan-Taylor polarizer (03PTA401; Melles Griot, Irvine, CA) was mounted as shown in Figure 3B into the center of a rigid wheel that could be rotated 260°. A rotary potentiometer in a voltage-divider circuit produced a voltage signal that varied linearly (between 0 and 5 V) with the angle of the prism. Light passing through the polarizer was collected with a photomultiplier (H957-06; Hamamatsu, Bridgewater, NJ). Photomultiplier output current was amplified with a custom-built preamp before connection to one of the pulse inputs of the electronics (25). Colored glass or interference filters were placed in front of the polarizer to select the appropriate fluorescence or scatter wavelengths.

For one experiment, data were collected by placing a 50% plate beamsplitter (03BTF007; Melles Griot) at 45° incidence in front of the polarizer. By convention, the plane of incidence for the beamsplitter is defined as that including the normal to the reflecting surface and the direction of the incident beam. *P*-polarized light refers to light polarized parallel to this plane of incidence and *s*-polarized refers to light polarized perpendicular to it. No beamsplitters were included in the detection path for any of the remaining experiments.

Sample Preparation

Fluorescent microspheres (Fluoresbrite YG, cat. no. 18860; Polysciences, Warrington, PA) were diluted 1:100 in distilled water prior to analysis. Mouse thymocytes were harvested from B10.PL(73NS)/Sn mice, centrifuged, and resuspended at $\sim 1 \times 10^6$ cells/ml in Dulbecco's phosphate-buffered saline (PBS, pH 7.1, cat. no. 14080-055; Gibco BRL, Gaithersburg, MD). The cytoplasmic dye, fluorescein diacetate (FDA, cat. no. 20164-2; Aldrich, Milwaukee, WI) was added, and the living cells were incubated for 30 min at 37°C and analyzed immediately. For labeling CD4 and CD8 cell surface receptors, the thymocytes were incubated with fluorophore-conjugated antibodies in staining buffer (PBS with 0.05% sodium azide and 5% fetal bovine serum) for 1.5 h at room temperature, washed twice by centrifugation, and then fixed by addition of 1% formaldehyde. Antibodies conjugated to fluorescein (anti-CD4-FITC) and phycoerythrin (anti-CD8-PE) were purchased from Pharmingen (cat. nos. 09424D and 01045B; San Diego, CA). The thiazole orange derivative, TO-PRO-1 iodide (TO), ethidium bromide (EB), propidium iodide (PI), TOTO-1 iodide (TOTO), ethidium-homodimer-1 (ETHD), and YOYO-1 iodide (YOYO) were incubated with thymocytes in PBS with added detergent (0.05% Triton-X to permeabilize membranes) and RNAse (50 μg/ml) for 30 min at room temperature prior to analysis. The DNA dyes were purchased from Molecular Probes (cat. nos. T-3602, E-3565, P-3566, T-3600, E-1169, and Y-3601; Eugene, OR). All procedures regarding the use of animals were approved by the Animal Care Committee at the University of Washington.

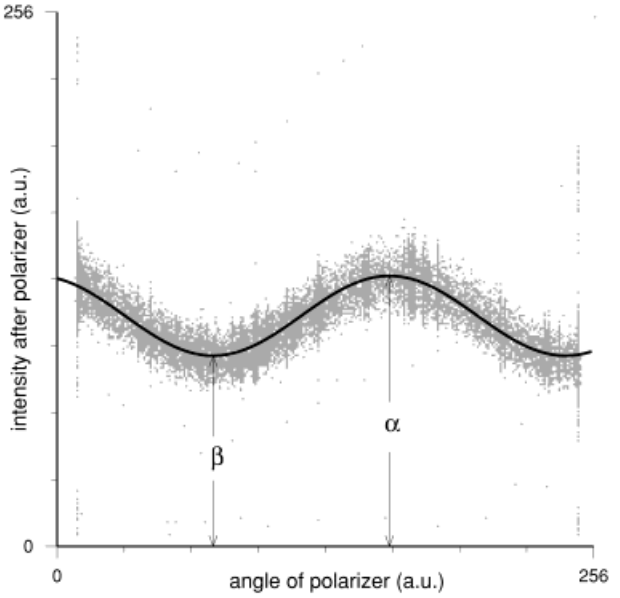

FIG. 4. Analysis of raw data from a polarization measurement. A bivariate dot-plot of 40,000 individual bead measurements is shown in gray. For every angle, a peak value was chosen after smoothing the intensity distribution with a 10-channel sliding window. As indicated by the black line, the resulting point pairs were fit with Equation 2 by adjusting α and β. Values of *P* could then be calculated by using α and β in Equations 16 and 17.

Measurement Procedure and Analysis

The polarizer was rotated manually during data acquisition. Both the angle of the polarizer and the light intensity collected after the polarizer were recorded for every measured particle. For each anisotropy calculation, a data list was collected including 40,000 particles distributed evenly over the 260° range of the rotating polarizer. A bivariate dot-plot of fluorescence intensity versus polarization angle for calibration beads shows the sinusoidal variation predicted by Equation 2 (Fig. 4). A vertical slice through Figure 4 at a given angle would reveal a distribution of intensities due to variation in particle brightness and to the overall precision limit of the system. In order to compress the raw data into a single curve, one intensity value was computed for each angle by taking the peak of the distribution after smoothing with a 10-channel sliding window. This process resulted in about 250 point pairs (angle x_n, intensity I_n) summarizing the dataset.

The Levenberg-Marquardt method of nonlinear least squares fitting (28) was used to compute the best-fit of Equation 2 to the point pairs. Four adjustable parameters were included in the fit. Two were the coefficients of $\cos^2\eta$ and $\sin^2\eta$, α and β, which were used to compute *P*. Two additional parameters, a gain and an offset, were needed to calibrate the angle measurement (i.e., to convert *x* in arbitrary units into η in degrees). New values for these two parameters were obtained each time the instrument was set up by measuring highly vertically polarized light and allowing the fitting routine to adjust all four parameters. For subsequent datasets, the same angle cali-

bration could be used by keeping the gain and offset fixed and allowing the fitting routine to adjust only α and β. The point pairs and best-fit curves for each dataset were normalized by dividing intensities by (α + β) and plotted in polar coordinates.

Uncertainties in the fitted parameters α and β were calculated by assuming that intensities were normally distributed around the best-fit curve and using the chi-square value as a measure of the width of the normal distribution (see ref. 28, p 661). Uncertainties in P were then calculated by standard propagation of error.

RESULTS

Verification of Polarization Theory Using Fluorescent Beads

Polar plots of intensity versus polarization angle for light scattered from uniform beads are shown in Figure 5. The measured intensity distributions followed Equation 2 very closely. Regardless of the direction of polarization of the laser, scattered light exhibited a very high degree of polarization, with values of $P > 0.83$. Scatter was perfectly polarized ($P \sim 1.00$) when the laser polarization was vertical (Fig. 5A), indicating that depolarized light from multiple reflections and aperture depolarization made a negligible contribution in this case. When the laser polarization was rotated, these depolarizing effects made a slightly more significant contribution, as indicated by the decrease in the degree of scatter polarization in Figures 5B and 5C.

Upon 488-nm excitation, the fluorescence from the beads was moderately polarized ($P = 0.194 \pm 0.003$; Fig. 6A). Repeated measurements (N = 28) of bead fluorescence at this excitation wavelength demonstrated excellent reproducibility (average $P = 0.189$, SD $\sigma_P = 0.011$). P values were independent of laser power (between 65 and 255 mW) and photomultiplier control voltage (between 0.2 and 0.6 V; data not shown). Unlike scatter, the main direction of fluorescence polarization did not rotate when the laser polarization was rotated (Figs. 6B,C). Only the degree of fluorescence polarization changed, decreasing toward $P \sim 0.00$ as the laser polarization became parallel with the detection axis (Fig. 6C). The degree of fluorescence polarization from these beads depended on the excitation wavelength. Upon UV excitation, bead fluorescence was only weakly polarized at $P = 0.052 \pm 0.002$ (data not shown).

Selection of Laser-Blocking Filters

It is important to completely block laser scatter in order to obtain accurate fluorescence polarization values for the beads. Figure 7 shows that the measured values changed depending on laser-blocking efficiency of a series of long-pass filters (500 through 550LP; Edmund Scientific, Barrington, NJ) and one rejection-band laser-blocking filter (488RB; Chroma Technology, Brattleboro, VT). A significant amount of 488-nm laser scatter leaked through the 500LP filter. In this case, the measured light was a superposition of scatter and fluorescence, resulting in a P value above the theoretical limit for fluorescence (P must be ≤ 0.5 for fluorescence). As filters were chosen with increasing (red-shifted) cut-on wavelengths, laser scatter was blocked more completely and measured values approached the true polarization of pure fluorescence from these beads. The 488RB filter blocked the laser very efficiently and had a very sharp cut-on at ~495 nm. Measurement with this filter gave the same value as with the 550LP.

Effects of Beamsplitters on Polarization Measurements

The effects of two different achromatic beamsplitters on polarization were investigated using fluorescence from calibration beads. The strong polarization sensitivity of a 50% plate beamsplitter is shown in Figure 8. When the mirror was placed in front of the polarizer at 45° incidence and oriented to reflect vertically, the transmitted light was more polarized than without the mirror (compare Fig. 8A to Fig. 6A). With the mirror oriented to reflect horizontally, the transmitted light was less polarized than without the mirror and exhibited a negative polarization. The ratio of transmission of *p*-polarized to *s*-polarized light for the 45° mirror was estimated to be $T_p/T_s = 1.64 \pm 0.05$ using the data from Figures 6A and 8A or 8B. A nonpolarizing cube beamsplitter had a weaker effect on the transmitted light, but still showed some polarization sensitivity ($T_p/T_s = 1.12 \pm 0.03$, data not shown).

Comparison of Our Method With Published Observations

Fluorescence polarization from living thymocytes loaded with FDA was measured at several different dye concentrations in isotonic media. Only a weak dependence on FDA concentration was observed (Fig. 9). Our values compare well with the measurements of Lindmo and Steen (7), and Deutsch et al. (16), but are higher than those of Epstein et al. (5) for the same medium tonicity. We discuss possible explanations for this discrepancy below.

Fluorescence Polarization of Commonly Used Dyes

In order to observe whether polarization happens under normal conditions in a flow cytometer, we studied several commonly used dyes. The degrees of fluorescence polarization for these dyes are shown in Table 1. Significant polarization was exhibited by all dyes tested. The degree of fluorescence polarization from the surface marker anti-CD4-FITC and all the DNA-bound dyes was high ($P \geq 0.25$). Figure 10 shows results for two different dyes. The high fluorescence polarization of EB is shown in Figure 10A and the low polarization of anti-CD8-PE is shown in Figure 10B.

DISCUSSION

Both the fluorescence and scatter induced by highly polarized light sources are anisotropic. The anisotropy of scatter has been recognized by some flow cytometrists, and has been found to be useful in discriminating between

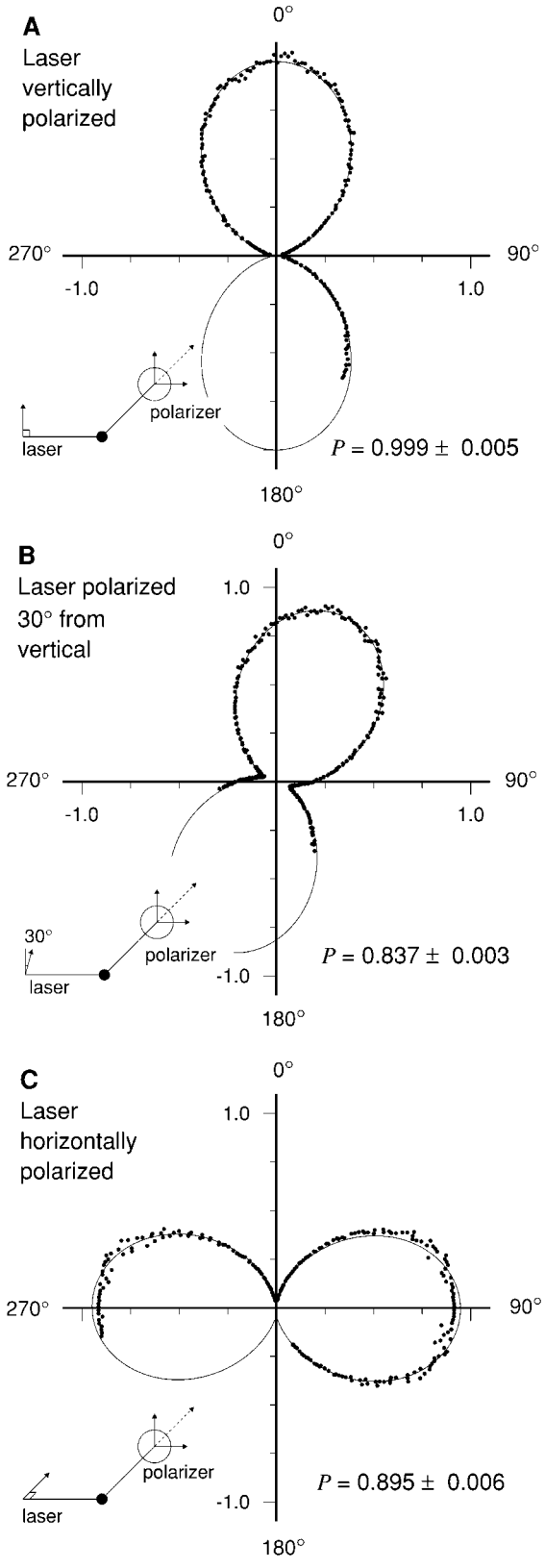

FIG. 5. Polar plots of relative intensity versus polarization angle for bead scatter. Curves show the best-fit of Equation 2 to the data points. **A:** Upon illumination with a vertically polarized, 488-nm laser, the light scattered from calibration beads was completely polarized. **B,C:** When the laser polarization was rotated 30° (B) and 90° (C) from vertical, the degree of polarization of scatter decreased slightly and the direction rotated with the laser. A band-pass interference filter (488BP10) was used to block bead fluorescence.

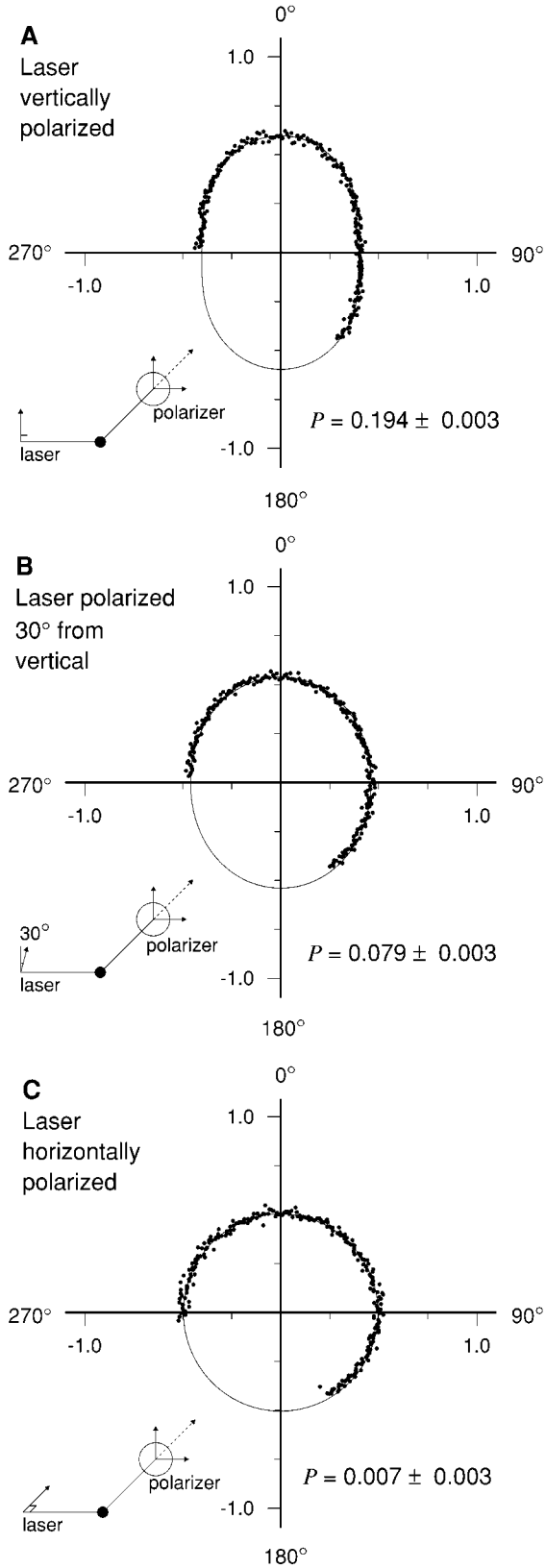

FIG. 6. Polar plots of relative intensity versus polarization angle for bead fluorescence. Curves show the best-fit of Equation 2 to the data points. **A:** Upon illumination with a vertically polarized, 488-nm laser, the fluorescence from calibration beads was moderately polarized. **B,C:** The degree of fluorescence polarization decreased as the laser polarization was rotated 30° from vertical (B). Measured fluorescence was not polarized when the laser polarization was 90° from vertical (C). Two laser-rejecting interference filters (488RB) were used to completely block laser scatter.

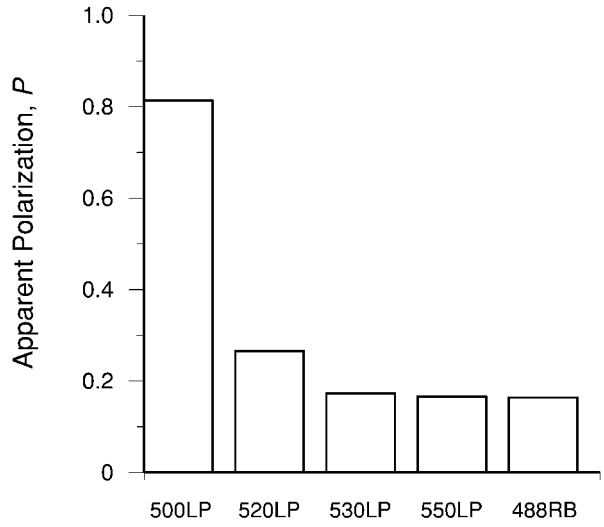

FIG. 7. Apparent fluorescence polarization of calibration beads measured through a series of filters with varying laser-blocking efficiency. With the long-pass 500LP filter, the polarization was far above the theoretical limit for fluorescence, indicating that 488-nm laser scatter was leaking through the filter. The 488RB laser-rejection filter blocked laser scatter very effectively while passing the greatest portion of fluorescence. The laser power (65 mW) and photomultiplier gain were identical for all the measurements.

certain cell types. In general, anisotropy of fluorescence is rarely considered despite the fact that it complicates the quantitation of fluorescence intensity and can defeat schemes for standardization of flow measurements. When pursuing quantitative measurements in flow, knowledge about the expected degree of fluorescence anisotropy is crucial.

We have presented a simple theory and a method to investigate the effects of anisotropy in typical flow cytometry experiments. We determined polarization state by rotating a polarizer in front of the detector. The orientation of the polarizer and the intensity passing the polarizer are recorded simultaneously. The polarizer is rotated during data collection. The distribution of intensity versus polarization angle for a population of particles is obtained. Intensity distributions are plotted in polar coordinates. A curve-fitting procedure is used to calculate the degree of polarization for the population.

This approach differs from previous methods (1,5,7,20,26), which used two detectors with orthogonal polarizers. Using two detectors allows determination of the degree of fluorescence polarization of signals from individual particles and the particles can be sorted on this basis. However, the two-detector method requires a priori knowledge of the main direction of polarization, because the polarizers must be oriented parallel and perpendicular to this cardinal direction. Furthermore, gain settings for the two independent channels must be balanced to ensure that the absolute detection efficiencies are equal. Our method precludes sorting, but is better suited to compare theoretical predictions with experimental observations. Balancing of the detector sensitivity is not required because only one detector is used. Complete distributions of intensity versus polarization angle are measured, so the main direction of polarization can be determined from the data. Consequently, the method can be used to measure the rotation of scatter polarization that is expected to occur with changes in observation angle. Complete intensity distributions also test theoretical predictions in detail.

Theory predicts that scatter and fluorescence differ markedly in the degree and direction of polarization. Scatter from a highly polarized laser will almost always have a high degree of polarization, often preserving the perfect polarization of the source. Fluorescence can also be polarized, but not to the same degree as scatter. With the orthogonal detection scheme common in most flow cytometers (i.e., with the detection axis perpendicular to the laser beam), rotating the laser polarization will cause the degree, but not the direction, of fluorescence polarization to change. Scatter will behave in just the opposite manner: the direction of scatter polarization will change as the laser is rotated, but a very high degree of polarization will be retained. Our measurements of calibration beads confirm these expectations (Figs. 5, 6). The measured intensity distributions for both fluorescence and scatter are fit very well by Equation 2. We therefore conclude that the theory developed above is applicable.

Based on results using a number of randomly selected dyes, our observations indicate that fluorescence polarization is a common phenomenon in flow cytometry (Table 1). The high degree of polarization observed for DNA dyes is expected. These dyes are rigidly bound to large, relatively immobile DNA molecules, so depolarization due to molecular movement should not occur. Besides molecular movement, however, depolarization can also occur through energy transfer. The lower polarization of dimeric DNA dyes (TOTO, ETHD, and YOYO) relative to monomeric dyes (TO, EB, and PI) suggests that intramolecular energy transfer occurs between the dimerized chromophores. Energy transfer may also be responsible for the very low polarization exhibited by the antibody-bound fluorophore, anti-CD8-PE, as compared to anti-CD4-FITC. These dyes are expected to have similar mobilities and fluorescence lifetimes, but unlike fluorescein (FITC), each PE molecule contains several closely linked fluorescent groups. Energy transfer may occur very readily between these groups.

To validate our method, we measured fluorescence polarization of mouse thymocytes loaded with FDA and compared our results with previous measurements (5,7,16). Our results generally agree with earlier measurements taken at similar dye concentration and medium tonicity (Fig. 9). Polarization values obtained by Epstein et al. (5) were lower, but this discrepancy could be explained by differences in incubation time, temperature, or differences between the cell types. It is believed that a fraction of intracellular fluorescein binds to cytoplasmic structures and that the remaining molecules float freely in the cell (6). Free molecules tumble during the lifetime of the excited state, and therefore emit fluorescence with little polarization. Bound molecules emit highly polarized

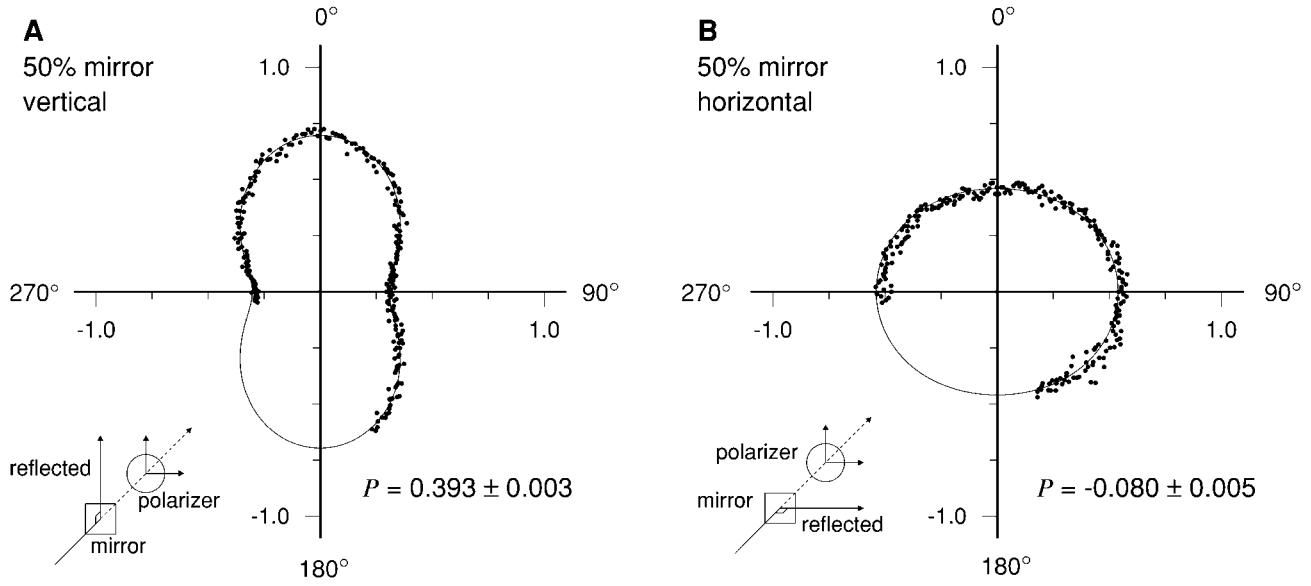

FIG. 8. Beamsplitters caused strong, orientation-dependent polarization artifacts. **A:** When a 50% mirror was placed at 45° incidence in the detection path and oriented to reflect upward (schematic, lower left), the measured polarization was higher than the true value (i.e., the value measured without a beamsplitter). **B:** When the mirror was oriented to reflect horizontally, the measured polarization was lower than the true value, becoming negative. These plots can be compared with Figure 6A, which shows the same measurement without a beamsplitter. A similar but less pronounced effect was measured using a nonpolarizing beamsplitter cube (data not shown).

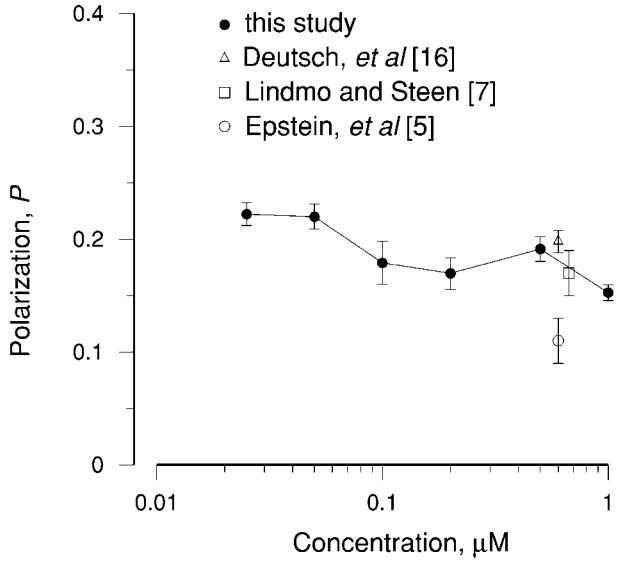

FIG. 9. Polarization of fluorescence from FDA-stained thymocytes. FDA fluorescence was excited with 488-nm light and collected through a combination of two laser-blocking filters (488RB) plus one long-pass filter (500LP). Our results (black circles) agree well with two previous measurements of intracellular fluorescein polarization at the same tonicity of the medium (open symbols). The discrepancy between our measurements and those of Epstein et al. (5) could be due to differences in equilibration time or may reflect variation between cell types (see Discussion).

Table 1
*Fluorescence Polarization of Thymocytes Stained With Various Dyes**

Dye	Target	Concentration	*P*
FDA	cytoplasm	0.5 μM	0.191 ± 0.011
CD4-FITC	cell surface	1:200*	0.235 ± 0.016
CD8-PE	cell surface	1:100*	0.041 ± 0.015
TO	DNA	1.25 μM	0.281 ± 0.001
EB	DNA	1.3 μM	0.323 ± 0.002
PI	DNA	3 μM	0.336 ± 0.004
TOTO	DNA	1.5 μM	0.133 ± 0.002
ETHD	DNA	1 μM	0.278 ± 0.002
YOYO	DNA	1 μM	0.126 ± 0.001

*Dilutions are given for the labeled antibodies because absolute concentrations were unknown.

fluorescence. Measured polarization values depend on the ratio of free to bound dye in the cell. Accordingly, Epstein et al. attributed a decrease in polarization during FDA incubation to saturation of binding sites as more of the dye was internalized. Considering this decrease in polarization with incubation time, it is not surprising that Epstein's measurement, made after a long (70 min) incubation, is the lowest in Figure 9. An alternative explanation for the disagreement is that the cell types used in each study may differ in number of intracellular dye-binding sites. In this case, polarization differences would persist even after long incubation times.

A serendipitous outcome of this work was the finding that polarization measurements could be used to test the laser-blocking efficiency of our filters. The polarization behaviors of scatter and fluorescence are very different. These differences provide sensitive criteria with which to determine whether laser scatter "leaks" through a colored filter. One approach (Fig. 7) is to compare the apparent degree of polarization of a particular source using several filters. Using a long-pass 500LP filter, the apparent polar-

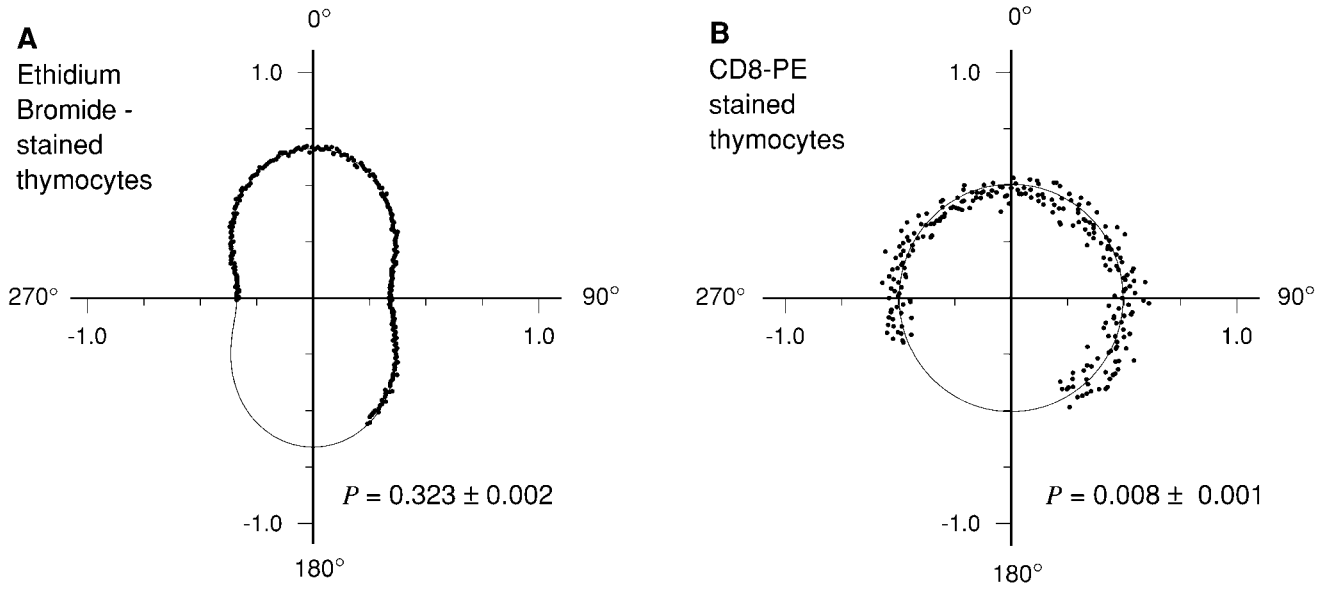

FIG. 10. Polarization of fluorescence of EB- and anti-CD8-PE-stained thymocytes. **A:** EB fluorescence was excited with 514-nm light and collected through a combination of one long-pass filter (550LP) and a neutral density filter. **B:** Anti-CD8-PE fluorescence was excited with 488-nm light and collected through a combination of two laser-blocking filters (488RB) and one long-pass filter (500LP) (Anti-CD8-PE antibody used at 1:200 dilution.). Photomultiplier gain and laser power (67 mW) were kept the same for both measurements.

ization of calibration beads was far above the theoretical limit for fluorescence (P must be ≤ 0.5, see Theory section), indicating that 488-nm laser scatter was leaking through the filter. The 488RB laser-rejection filter blocked laser scatter very effectively while passing the greatest portion of fluorescence. The trend for longer (redder) cut-on wavelengths to give lower polarization is mostly due to differences in the laser-blocking efficiency of this series of filters, because polarization measured with the 488RB filter was the same as with the 550LP. The alternative explanation, that the polarization of these beads varies across the fluorescence spectrum, is not likely. This is because the transmission spectrum of the 488RB closely resembles that of the 500LP, but with a much sharper cut-off below 500 nm (data not shown). Another, perhaps simpler, technique for determining laser-blocking efficiency would be to measure the apparent polarization direction, rather than the degree, of a particular source as the laser polarization is rotated. As demonstrated above, the polarization direction of pure fluorescence will not change, so that any change in the apparent polarization direction indicates that scatter is leaking through the filter. A quantitative measure of laser-blocking efficiency for specific filter combinations could be obtained from such data. Such a measure would allow objective evaluation of filter sets.

Although some cytometrists have deliberately used fluorescence polarization as a tool, it is usually ignored despite the fact that it significantly impacts schemes for instrument calibration and standardization, which have received a great deal of attention. (The entire October 1, 1998 issue of *Cytometry* was devoted to the subject.) Unless special care is taken, all flow cytometers are polarization sensitive. Beamsplitters used often in cytometry have transmissivities that depend strongly on the polarization state of the incident beam and on the orientation of the splitter with respect to the direction of polarization. The plate beamsplitter analyzed in Figure 8 transmitted *p*-polarized light 64% more efficiently than *s*-polarized light. Although not measured here, dichroic beamsplitters are expected to have similar polarization sensitivity. A so-called nonpolarizing beamsplitter cube exhibited a 12% difference in transmission between the *s*- and *p*-polarizations (data not shown). Even in simple systems without beamsplitters, polarization sensitivity persists because emission from a polarized source is not the same in all directions. The emitted intensity in the direction of the detector depends not only on the total brightness, but also on the degree of anisotropy. Two particles that emit exactly the same amount of light, but with different degrees of anisotropy, will not emit the same intensity toward the detector.

Although one might expect otherwise, this artifact cannot be avoided by using a circularly polarized laser or a light beam from an unpolarized lamp. Whereas using a circularly or randomly polarized excitation beam will reduce the degree of fluorescence anisotropy, it will not completely eliminate it. A better approach is to construct an instrument that is not sensitive to the degree of anisotropy, taking advantage of the magic angle. This can be achieved in either of two ways. First, a polarizer with its pass-axis oriented at 54.7° with respect to the direction of laser polarization can be placed between the source and the detection optics. A second option is to rotate the laser polarization so that it makes an angle of 54.7° with the detection axis. These steps will reduce signal intensity,

but the measured intensity will be proportional to the total emission and will not be influenced by emission anisotropy.

Considering that cytometry samples differ in polarization and that cytometers can differ in polarization sensitivity, schemes for calibration and standardization of fluorescence measurements based only on intensity ratios may lead to erroneous conclusions about relative dye content. Several recent efforts toward interlaboratory standardization of cytometry measurements were based entirely on intensity ratios between labeled cells and reference beads. Although the different laboratories generally agreed on the fluorescence ratios between beads of a particular series (30), the reproducibility was much poorer for measurements of the antibody-binding capacity of cells (29–32). Of the many possible explanations for this poor reproducibility, anisotropy is a good candidate that is not acknowledged in any of the studies. If machines that vary in polarization sensitivity were used to compare samples with different anisotropies (e.g., beads versus labeled cells), they would not give the same intensity ratios. A series of calibration beads (of the same type, but varying in size) would exhibit identical anisotropies, so ratios between the beads would not depend on the polarization sensitivity of the machine (33). It is possible that anisotropy makes a significant contribution to the 20–30% interlaboratory variation that typically occurs when measuring antibody-binding capacity by a ratio method. This possibility must be investigated carefully before quantitative fluorescence cytometry (QFCM) can be regarded as a realistic goal.

LITERATURE CITED

1. Arndt-Jovin DJ, Ostertag W, Eisen H, Klimek F, Jovin TM. Studies of cellular differentiation by automated cell separation. Two model systems: Friend virus-transformed cells and *Hydra attenuata*. J Histochem Cytochem 1976;24:332–347.
2. Arndt-Jovin DJ, Jovin TM. Cell separation using fluorescence emission anisotropy. In: Marchesi VT, ed. Membranes and neoplasia: new approaches and strategies. New York: Alan R. Liss; 1976. p123–136.
3. Chan SS, Arndt-Jovin DJ, Jovin TM. Proximity of lectin receptors on the cell surface measured by fluorescence energy transfer in a flow system. J Histochem Cytochem 1979;27:56–64.
4. Dix JA, Verkman AS. Mapping fluorescence anisotropy in living cells by ratio imaging. Application to cytoplasmic viscosity. Biophys J 1990;57:231–240.
5. Epstein M, Norman A, Pinkel D, Udkoff R. Flow system fluorescence polarization measurements on fluorescein diacetate-stained EL4 cells. J Histochem Cytochem 1977;25:821–826.
6. Kinoshita S, Fukami T, Ido Y, Kushida T. Spectroscopic properties of fluorescein in living lymphocytes. Cytometry 1987;8:35–41.
7. Lindmo T, Steen HB. Flow cytometric measurement of the polarization of fluorescence from intracellular fluorescein in mammalian cells. Biophys J 1977;18:173–187.
8. Beisker W, Eisert WG. Denaturation and condensation of intracellular nucleic acids monitored by fluorescence depolarization of intercalating dyes in individual cells. J Histochem Cytochem 1989;37:1699–1704.
9. Collins JM, Grogan WM. Comparison between flow cytometry and fluorometry for the kinetic measurement of membrane fluidity parameters. Cytometry 1989;10:44–49.
10. Collins JM, Dominey RN, Grogan WM. Shape of the fluidity gradient in the plasma membrane of living HeLa cells. J Lipid Res 1990;31:261–270.
11. Collins JM, Scott RB, Grogan WM. Plasma membrane fluidity gradients of human peripheral blood leukocytes. J Cell Physiol 1990;144:42–51.
12. Dynlacht JR, Fox MH. Heat-induced changes in membrane fluidity of Chinese hamster ovary cells measured by flow cytometry. Radiat Res 1992;130:48–54.
13. Dynlacht JR, Fox MH. The effect of 45°C hyperthermia on the membrane fluidity of cells of several lines. Radiat Res 1992;130:55–60.
14. Fox MH, Delohery TM. Membrane fluidity measured by fluorescence polarization using an EPICS V cell sorter. Cytometry 1987;8:20–25.
15. Jacobsen PB, Stokke T, Solesvik O, Steen HB. Temperature-induced chromatin changes in ethanol-fixed cells. J Histochem Cytochem 1988;36:1495–1501.
16. Deutsch M, Ron I, Weinreb A, Tirosh R, Chaitchik S. Lymphocyte fluorescence polarization measurements with the cellscan system: application to the SCM cancer test. Cytometry 1996;23:159–165.
17. Scott RB, Collins JM, Hunt PA. Alzheimer's disease and Down syndrome: leukocyte membrane fluidity alterations. Mech Ageing Dev 1994;75:1–10.
18. Jerlov NG. Marine optics. Amsterdam: Elsevier; 1976.
19. van den Engh GJ, Visser J. Light scattering properties of pluripotent and committed haemopoietic stem cells. Acta Haematol 1979; 62:289–298.
20. de Grooth BG, Terstappen LWMM, Puppels GJ, Greve J. Light-scattering polarization measurements as a new parameter in flow cytometry. Cytometry 1987;8:539–544.
21. Cantor CR, Schimmel PR. Biophysical chemistry part II: techniques for the study of biological structure and function. San Francisco: WH Freeman; 1980. p 455–465.
22. Thomas GB, Finney RL. Calculus and analytical geometry, 6th edition. Reading, MA: Addison-Wesley; 1984.
23. Swaminathan R, Hoang CP, Verkman AS. Photobleaching recovery and anisotropy decay of green fluorescent protein GFP-S65T in solution and cells. Biophys J 1997;72:1900–1907.
24. Asbury CL, Esposito R, Farmer C, van den Engh GJ. Fluorescence spectra of DNA dyes measured in a flow cytometer. Cytometry 1996;24:234–242.
25. van den Engh GJ, Stokdijk W. Parallel processing data acquisition system for multilaser flow cytometry and cell sorting. Cytometry 1989;10:282–293.
26. Pinkel D, Epstein M, Udkoff R, Norman A. Fluorescence polarimeter for flow cytometry. Rev Sci Instrum 1978;49:905–912.
27. van den Engh GJ, Farmer C. Photo-bleaching and photon saturation in flow cytometry. Cytometry 1992;13:669–677.
28. Press WH, Teukolsky SA, Vetterling WT, Flannery BP. Numerical recipes in C: the art of scientific computing, 2nd edition. Oxford: Cambridge University Press; 1992.
29. Gratama JW, D'hautcourt JL, Mandy F, Rothe G, Barnett D, Janossy G, Papa S, Schmitz G, Lenkei R. Flow cytometric quantitation of immunofluorescence intensity: problems and perspectives. Cytometry 1998;33:166–178.
30. Waxdall MJ, Monical MC, Palini AG. Inter-laboratory relative fluorescence intensity measurements using FlowCal 575 calibration beads: a baseline study. Cytometry 1998;33:213–218.
31. Bergeron M, Faucher S, Minkus T, Lacroix F, Ding T, Phaneuf S, Somorjai R, Summers R, Mandy F. Impact of unified procedures as implemented in the Canadian Quality Assurance Program for T lymphocyte subset enumeration. Cytometry 1998;33:146–155.
32. Zenger VE, Vogt R, Mandy F, Schwartz A, Marti GE. Quantitative flow cytometry: inter-laboratory variation. Cytometry 1998;33:138–145.
33. Kerker M, Van Dilla MA, Brunsting A, Kratohvil JP, Hsu P, Wang DS, Gray JW, Langlois RG. Is the central dogma of flow cytometry true: that fluorescence intensity is proportional to cellular dye content? Cytometry 1982;3:71–78.